Heliyon 6 (2020) e04165

Contents lists available at ScienceDirect

Heliyon

journal homepage: www.cell.com/heliyon

Research article

Tight expression regulation of senataxin, linked to motor neuron disease and ataxia, is required to avert cell-cycle block and nucleolus disassembly

Craig L. Bennett [a,*,1], Bryce L. Sopher [b], Albert R. La Spada [a,c,d,e]

[a] Department of Neurology, Duke University School of Medicine, Durham, NC 27710, USA
[b] Department of Neurology, University of Washington Medical Center, Seattle, WA 98195, USA
[c] Department of Neurobiology, Duke University School of Medicine, Durham, NC 27710, USA
[d] Department of Cell Biology, Duke University School of Medicine, Durham, NC 27710, USA
[e] Duke Center for Neurodegeneration & Neurotherapeutics, Duke University School of Medicine, Durham, NC 27710, USA

ARTICLE INFO

Keywords:
Cell biology
Genetics
Neuroscience
Infectious disease
Gene expression
Gene regulation
Mutation
Senataxin
Helicase
Fibrillarin
ALS4
Nucleolus
Ataxia

ABSTRACT

The Senataxin (SETX) protein exhibits strong sequence conservation with the helicase domain of the yeast protein Sen1p, and recessive *SETX* mutations cause a severe ataxia, known as Ataxia with Oculomotor Apraxia type 2, while dominant *SETX* mutations cause Amyotrophic Lateral Sclerosis type 4. SETX is a very low abundance protein, and its expression is tightly regulated, such that large increases in mRNA levels fail to significantly increase protein levels. Despite this, transient transfection in cell culture can boost SETX protein levels on an individual cell basis. Here we found that over-expression of normal SETX, but not enzymatically-dead SETX, is associated with S-phase cell-cycle arrest in HEK293A cells. As SETX interacts with the nuclear exosome to ensure degradation of incomplete RNA transcripts, and SETX localizes to sites of collision between the DNA replication machinery and the RNAP II complex, altered dosage or aberrant function of SETX may impede this process to promote S-phase cell-cycle arrest. Because neurons are enriched for long transcripts with additional antisense regulatory transcription, collisions of RNAP II complexes may occur in such post-mitotic cells, underscoring a role for SETX in maintaining neuron homeostasis.

1. Introduction

The study of *SETX* is of significant clinical interest, as recessive loss-of-function mutations cause a severe ataxia, known as Ataxia with Oculomotor Apraxia type 2 (AOA2; OMIM: 606002). More than 150 different *SETX* mutations have been identified to date, Human Gene Mutation Database (*HGMD*) [1], and the majority of these are loss-of-function mutations found in patients with AOA2. Unlike related ataxias, such as ataxia-telangiectasia (A-T) [2], AOA2 patients do not display an increased risk of cancer [3], suggesting that SETX is not directly involved in canonical DNA damage repair pathways. Interestingly though, both AOA2 and A-T patients show elevated serum levels of alpha-feto-protein [4], the most abundant fetal plasma protein.

Dominant *SETX* mutations also cause a juvenile-onset form of familial Motor Neuron Disease (MND), known as ALS4 [5]. ALS4 is unusual in that it is non-fatal, shows symmetrical distribution, and has little to no bulbar involvement [6]. ALS4-linked mutations are rare, with the L389S substitution located in the 'protein interaction domain' reported in at least three independent pedigrees with similar motor-specific phenotypes [5, 7, 8]. In one large American pedigree, > 50 affected members segregate the L389S mutation, confirming its pathogenicity [9]. ALS4-linked mutations likely act through a toxic gain-of-function mechanism, as AOA2 heterozygous carriers do not develop neurologic disease and remain symptom-free with age [10].

SETX is a large 2,677 amino acid (aa) protein defined by one highly conserved helicase domain (residues 1931–2456), with homology to only two other human proteins, Rent1 and IGHMBP2. Rent1 is an essential component of the nonsense-mediated RNA decay (NMD) complex [11], and recessive mutations of the *IGHMBP2* gene cause a fatal disorder, Spinal Muscle Atrophy with Respiratory Distress (SMARD) [12]. Studies suggest that SETX may aid in the resolution of R-loops that form when newly transcribed RNA hybridizes back to the coding DNA strand [13,

* Corresponding author.
E-mail address: cbennett@lincoln.ac.uk (C.L. Bennett).
[1] Current address: University of Lincoln; Lincoln, Lincolnshire LN6 7DL, United Kingdom.

https://doi.org/10.1016/j.heliyon.2020.e04165
Received 12 April 2020; Received in revised form 7 May 2020; Accepted 4 June 2020

14]. However, the significance of SETX-mediated R-loop resolution in neurodegenerative disease remains unknown. *Setx* knock-out mice exhibit no obvious R-loop resolution abnormalities in the cerebellum or brain [15], and various assays suggest that SETX absence produces only modest if any effects on transcription termination [16].

A growing body of evidence suggests that SETX forms nuclear foci during the S/G_2 transition phase of the cell-cycle, indicative of replication stress at collision sites between the DNA replisome and transcription machinery [17, 18]. Indeed, such nuclear foci are reduced by transcription inhibition and increased by impaired DNA replication [18]. There is also evidence that SETX has retained a link to the nuclear RNA exosome, as we and others have documented that SETX binds to Exosc9 [19,20], and shown that SETX co-depletion occurs when Exosc9 or Exosc10 are depleted [20]. SETX also appears to be regulated by the sumoylation pathway [19], as SUMO modification is required for SETX interaction with the RNA exosome [20]. SETX may perform a related function in G_0 neurons to those delineated within cycling cells. For example, RNA Polymerase II (RNAP II) undergoes self-collision in regions where positive strand and negative strand transcription overlaps [21], including where non-coding regulatory RNAs are transcribed in the antisense direction. A role for SETX at sites of RNAP II collisions may prove particularly important for active neurons as part of the aging process, given the large number of long brain-specific transcripts [22].

SETX is a very low-abundant protein with <500 molecules/cell, similar to its homologue, IGHMBP2 [23]. Protein levels of SETX and its yeast homologue, Sen1p, are tightly regulated, such that large increases in mRNA levels fail to significantly increase protein levels [24, 25]. Despite this, transient transfection in cell culture can boost SETX protein levels on an individual cell basis. Here we examined the subcellular localization of GFP- and Flag-tagged SETX in HEK293 cells, and found that SETX showed localization to the nucleoplasm. However, when we co-stained for the nucleolus markers fibrillarin or B23, they both displayed diffuse redistribution from the nucleolus to the nucleoplasm upon SETX over-expression. This redistribution occurred at a frequency as high as 90% at 24- and 72-hours post-transfection, regardless of whether the epitope tag was GFP or Flag. Importantly, enzymatically dead SETX had no effect on nucleolus marker localization. While we observed dissolution of the nucleolus in cells over-expressing SETX, recombinant SETX itself remained in the nucleoplasm. By monitoring cell-cycle progression using propidium iodide and flow cytometry, we were able to attribute this phenomenon to a block in cell-cycle progression.

2. Material & methods

2.1. SETX expression constructs

We created a GFP-tagged SETX construct for subcellular localization studies. Full cloning details of our original Flag-tagged SETX construct were outlined previously [26]. To generate a GFP tagged SETX construct we PCR amplified eGFP from an eGFP Clontech vector. The upstream primers contained a 5′-prime extension that encoded FLAG tag. The downstream primer contained the *Not* I site. In a second amplification step, an extension primer is used to add the additional Flag tags and includes a *Nhe* I for ease of cloning. Finally we took the re-derived 3xFlag-GFP containing eGFP vector and digested out the entire CMV 3xFlag-eGFP-Flag-SETX segment by *Kpn* I/*Mlu* I digestion and ligated this into the same restriction enzyme sites of our previously reported Flag-SETX construct [26]. For the mini-SETX construct, the eGFP coding sequence was inserted into our existing Flag-SETX construct at *Bgl* II restriction enzyme sites. This represents an internal deletion of 1114 residues from the SETX protein (residues 717 to 1831), which was replaced with 231 residues of eGFP. This means that the mini-SETX construct still retains the N-terminus domain (residues 1–500) [5]; (ii) the helicase domain (residues 1931–2456) [5] and the Nuclear Localization Signal (residues 2661–2677) [26]. The P-LoopΔ-SETX construct was generated using the Gibson Assembly Cloning Kit (NE BioLabs™) to affect an eight amino acid deletion (GPPGTGKS) of the SETX GTP/ATP binding domain. We PCR amplified Chloramphenicol selection cassette and incorporated SETX targeting sequence either side of the deletion region along with *Asc* I 8-bp restriction sites not present in our Flag-SETX construct. The final step involved *Asc* I digestion, following by DNA ligation to delete out the P-Loop and replace it with one *Asc* I site and a single T base to maintain the correct coding frame. All constructs generated by our group were validated by DNA Sanger sequencing.

2.2. Cell culture and transfections

HEK293A and HeLa cells were grown in DMEM media with 10% FBS. In all transfections with SETX constructs, endogenous SETX was still present in the cell culture. Transfections were performed using Lipofectamine 2000, according to the manufacturer's instructions (Invitrogen). The media was replaced after 4 h. Hek293A cells were not synchronized prior to cell cycle analysis.

Transfections efficiency with SETX based expression constructs were relatively low. The SETX open reading frame (orf) is large at 8034-bp. Thus, transfection efficiency based upon all SETX expression constructs (GFP-SETX, Flag-SETX, GFP-mini-SETX and Flag-P-loopΔ-SETX) were ~30% based upon fluorescent microscopy and random field counting.

2.3. Immunocytochemistry

Cells were seeded into 24-well plates containing glass circle cover slips (Thermo Fisher) prior to experimentation. Cells were transfected when ~50% confluent as indicated. PBS-MC buffer was used for all washes and as a diluent for all solutions. Cells were fixed with 4% paraformaldehyde in PBS-MC for 21-min. Cells were permeabilized for 5-min in 0.2% Triton-X in PBS, then placed in blocking solution (5% Normal Goat Serum and 5% BSA in PBS) for 1-hr. Primary and secondary antibodies were diluted in 5% normal goat serum in PBS-MC. Cells were incubated with primary Ab's O/N at 4 °C. Cells were washed with PBS-MC and then incubated in secondary Ab's for 1-hr. Next, cells were counter stained with a 1:20,000 solution of DAPI in PBS for 10-min. Finally, cover slips were washed once with PBS-MC and mounted on slides. Images were captured with a Zeiss LSM 780 confocal microscopy and analyzed with Zen 2011 LSM 780 software. Ab's used include: (i) fibrillarin mAb (Gene Tex: GTX24566); B23 mAb (ProteinTech: 60096-1); Flag mAb (Sigma: F3165); fibrillarin rabbit-Alexa 488 conjugate (Cell Signaling: C13C3).

2.4. PI staining for FACS analysis

A 6-cm petri dish of confluent Hek293A cells were harvested 24-hr after GFP transfection and washed with 2 ml of ice-cold PBS. Cell were fixed in -20 °C 70% ethanol for 30-min, with mild vortexing every 10-min to prevent cells from clumping. Fixed cells were centrifuged at 2000-rpm for 5-min and washed a further two times with 1-ml of PBS. Cells were then re-suspended in 800μl PI staining solution at 4 °C for 20-min in the dark. Samples with filtered with a 35μm nylon mesh snap/cap tube prior to loading onto the BD LSR Fortessa instrument.

2.5. Statistical analysis

All data were prepared for analysis with Microsoft Excel. Statistical analysis was done using Microsoft Excel or Prism 4.0. For ANOVA, if statistical significance ($P < 0.05$) was achieved, we performed post-hoc analysis to account for multiple comparisons. For the analysis of Fibrillarin and B23 being localized distinctly to the nucleolus or the nucleoplasm (Figure 2B), we performed three distinct transfections. Thereafter, we pooled the results for a total count of $n \geq 50$ for GFP-SETX positive, GFP-mini-SETX positive, or non-transfected cells respectively.

3. Results

3.1. SETX over-expression in HEK293A cells linked with nucleolus dissolution

To track SETX subcellular localization, we developed a GFP-tagged, full-length expression construct. We tested if SETX might show nucleolus localization, based upon initial yeast Sen1p experimentation [26, 27]. There is growing interest in the nucleolus, as disruption of this structure has been implicated in ALS linked to mutations in various RNA-binding proteins and C9orf72 dipeptide repeats [28, 29]. We transiently transfected HEK293A cells with GFP-SETX and found nucleoplasm localization (Figure 1A). Unexpectedly, in the vast majority of transfected cells, fibrillarin redistributed from the nucleolus to the nucleoplasm just 24 h after transfection (Figure 1A). We then examined the marker B23 as a sensitive marker of nucleolus toxicity [30]. We found that with GFP-SETX transfection, B23 was similarly redistributed from the nucleolus to the nucleoplasm (Figure 1B). We found no evidence of apoptosis mediated cell death such as chromosome condensation, nor any evidence of cellular morphological changes linked with GFP-SETX transfection.

To rule out GFP artifacts, we developed a GFP 'mini-SETX' control containing a large 1114 amino acid internal deletion, replaced with the GFP coding region. GFP-mini-SETX transfection showed partial mislocalization to the cytosol (Figure 2A), and failed to disrupt nucleolar appearance (Figure 2A). To measure the frequency of nucleolar to nucleoplasm marker redistribution, we performed three independent transfections with the following constructs: (i) GFP-SETX; (ii) GFP-mini-SETX; and (iii) non-transfected control. We counted at least 50 GFP-positive cells counterstained for fibrillarin or B23, as well as 50 non-transfected control cells. Non-transfected cells showed a normal nucleolar staining pattern for B23 and fibrillarin at 97% and 99% respectively. For GFP-SETX, the B23 and fibrillarin nucleolus staining appeared normal in only 10% of transfected cells. However, for GFP-mini-SETX transfected cells, nucleolus staining appeared normal for B23 in 88% of cells and for fibrillarin in 93% of cells (Figure 2B). Although the percentage of cells with B23 and fibrillarin distinctive nucleolus staining was dramatically reduced in GFP-SETX transfected cells compared with controls ($P < 0.01$), GFP-mini-SETX transfected cells were comparable to non-transfected controls (Figure 2B).

3.2. SETX disruption of the nucleolus requires an intact helicase domain

For further controls, we transfected both GFP-SETX and Flag-SETX into HEK293A cells, and observed that over-expression of SETX results in disruption of the nucleolus, regardless of the epitope tag (Figure 3A). To determine if SETX disassembly of the nucleolus was simply due to random proteotoxicity, we derived a helicase-dead version of SETX by deleting eight residues (p.1963–1970) that comprise the P-Loop GTP/ATP binding motif [5], and found that transfection of HEK293A cells with P-LoopΔ-SETX did not affect fibrillarin nucleolar localization (Figure 3B). Quantification of fibrillarin and B23 in transfected cells as represented in Figures 3A – 3B, were treated similarly as depicted in Figure 2B (see methods). Taken together, these results indicate that: (i) SETX induced disruption of the nucleolus is not dependent on the GFP tag; (ii) nucleolus disruption is dependent upon an active SETX helicase domain; and (iii) P-LoopΔ-SETX, like GFP-mini-SETX, shows occasional mislocalization to the cytosol (white arrows, Figure 3B). This is a phenomena unrelated to lack of SETX as treatment of cell culture with siRNA to deplete SETX protein levels [25], has no impact on B23 staining or nucleolus linked, cell-cycle progression (**data not shown**).

3.3. SETX disassembly of the nucleolus is linked with cell-cycle arrest

We considered two possible explanations for SETX induced nucleolus disassembly, as follows: (i) elevated SETX levels are toxic to the nucleolus in a manner similar to that of C9orf72 repeat expansion associated GR or PR dipeptides [28, 29]; or (ii) elevated SETX levels may induce an S-phase cell-cycle block [31]. DAPI nuclear staining did not reveal any evidence for increased apoptosis in GFP-SETX transfected cells even after 72 h of transfection. In addition, we noted that the typical prophase related nucleolus marker redistribution in a small percentage of

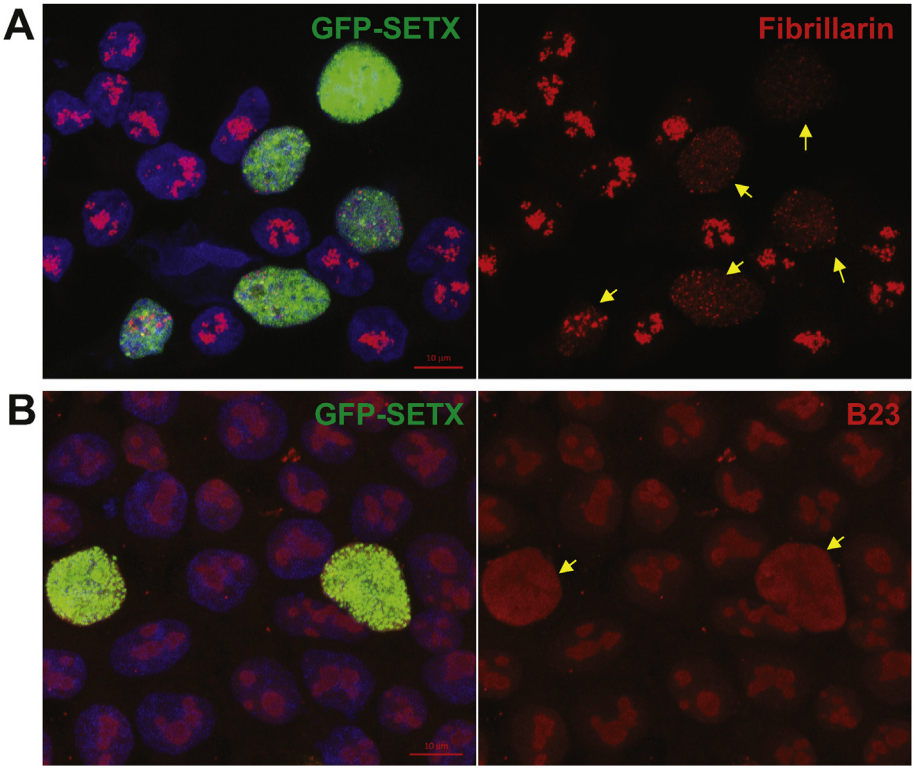

Figure 1. SETX over-expression in HEK293A cells results in the redistribution of nucleolus markers fibrillarin and B23. (A) HEK293A cells were transfected with GFP-SETX (green) and 24 h later cells were immunostained with anti-fibrillarin Ab (red) which marks the nucleolus and DAPI (blue) to define the nucleus. Yellow arrows indicate fibrillarin signal dispersed throughout the nucleoplasm in cells expressing recombinant SETX. Scale bar = 10μM. (B) The nucleolus marker B23 (red) was also seen as diffuse signal throughout the nucleoplasm, coincident with GFP-SETX expression. Scale bar = 10μM.

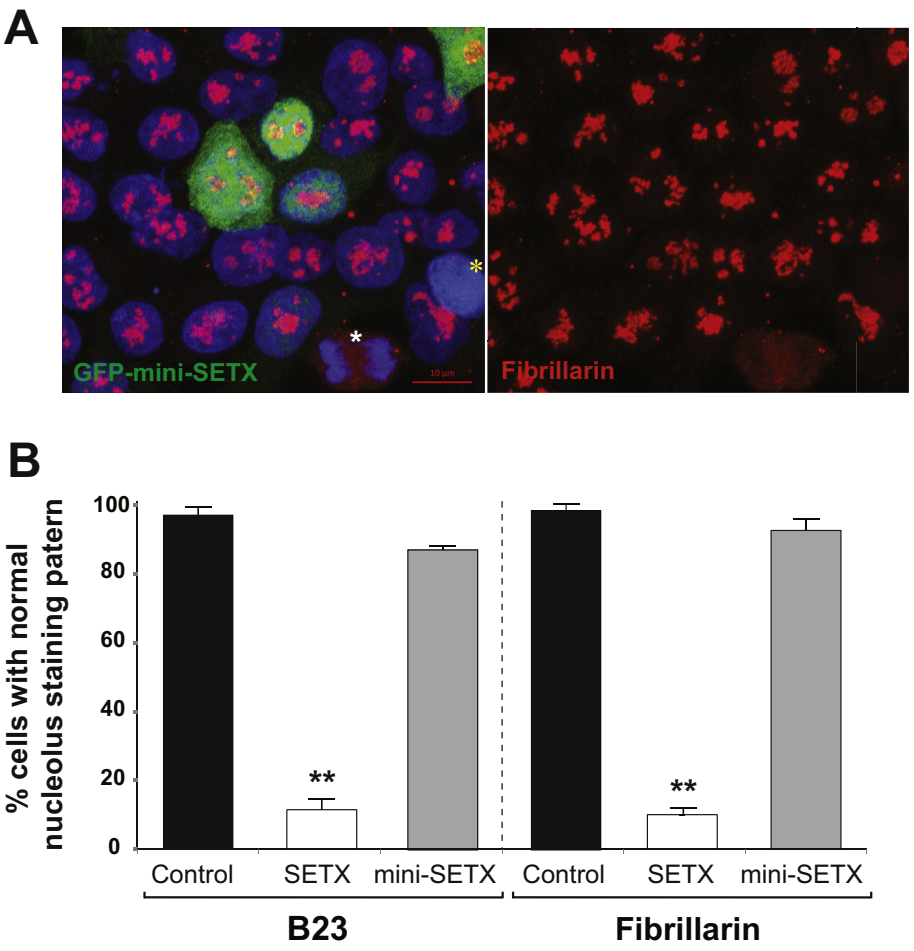

Figure 2. GFP-mini-SETX expression in HEK293A cells does not perturb the nucleolus, and GFP-SETX, but not by GFP-mini-SETX, is linked with nucleolus disassembly. (A) HEK293A cells were transfected with GFP-mini-SETX, and immunostained with anti-fibrillarin Ab (Red). Note that cells clearly positive for GFP (mini-SETX) show a normal fibrillarin nucleolus staining pattern. Rare exceptions include one cell in G_2/mitosis (white asterisk) and a second cell that is weakly GFP positive but is likely entering S-phase (yellow asterisk). Scale bar = 10μM. (B) To gauge frequency, we repeated the GFP-SETX(SETX) and GFP-mini-SETX(mini-SETX) transfections three times and counted at least 50 GFP-positive cells. For untransfected cells, B23 and fibrillarin showed normal nucleolar staining 97% and 99% of the time, respectively. For GFP-mini-SETX transfected cells, B23 and fibrillarin showed normal nucleolar staining 88% and 93% of the time, respectively. However, for GFP-SETX transfected cells, B23 and fibrillarin showed a normal nucleolus staining pattern only 10% of the time for both markers. $^{**}P < 0.01$; ANOVA with post-hoc Tukey test, while GFP-mini-SETX was not significantly different versus control.

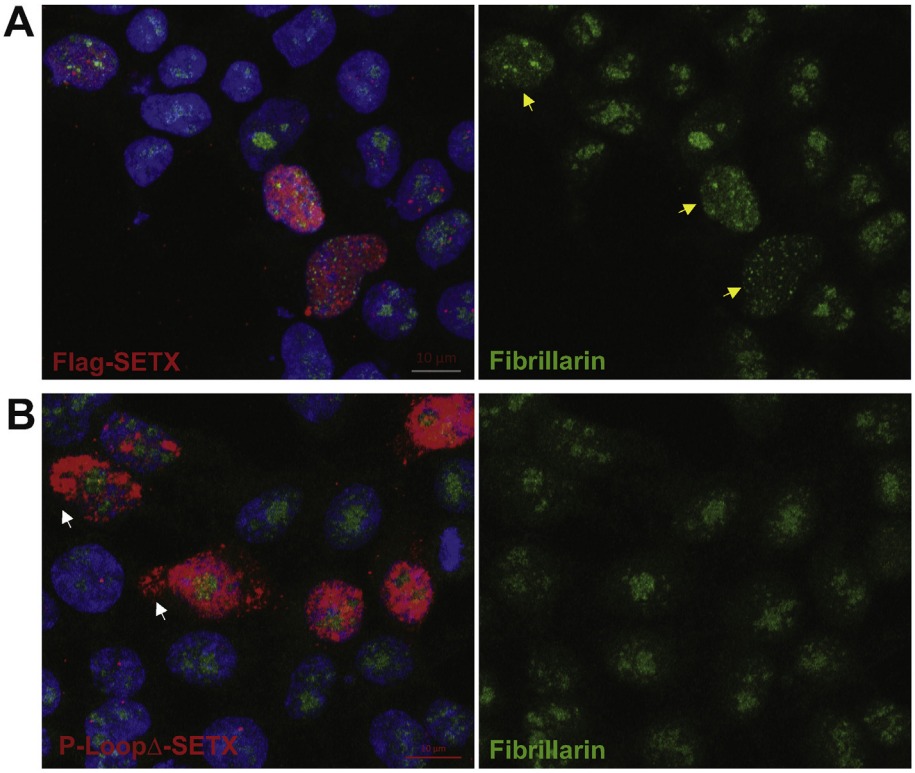

Figure 3. Flag-SETX expression in HEK293A cells linked with nucleolus dissolution, while helicase-dead SETX is not. (A) HEK293A cells were transfected with Flag-SETX and immunostained with anti-Flag antibody (red) 24 h after transfection. Fibrillarin signal was detected with the rabbit Alexa-488 conjugate antibody (green). Cells transfected with Flag-SETX show disassembly of the nucleolus (yellow arrows). Scale bar = 10μM. (B) HEK293A cells were transfected with P-LoopΔ-SETX (deletion p.1963-p.1970) which lacks the ATP/GTP binding domain, and 24 h later cells were prepared for anti-fibrillarin-488 (green) and anti-Flag (red) antibody visualization. Scale bar = 10μM.

non-transfected cells (Figure 2A, yellow asterisk), was very similar to what we saw in the majority of SETX transfected cells. To test if SETX over-expression interferes with cell cycle progression, we repeated the transfection experiment and performed propidium iodide (PI) staining and flow cytometry. GFP-negative signal was defined from non-transfected cells. 133,759 total events were sorted from GFP-SETX transfected Hek293A cells to remove cell debris and cell doublets with forward-scatter (P1, 18%) and side-scatter (P2, 2%) gating to isolate viable single cells (P3) = 107,136. The PI signal (675/25BP) was plotted for 70,869 GFP-negative cells. 10,000 GFP-positive cells (GFP^+) were gated and PI signal was plotted. When we compared GFP-SETX transfected versus for non-transfected (GFP negative) cells within the same culture, we noted a marked reduction in the percentage of G_1 cells (~29% vs. ~47% for non-transfected cells) and a dramatic increase in the percentage of cells in S-phase (~62% vs. 34% for non-transfected cells), based upon plotting of the PI signal (Figure 4). The percentage of cells in G2/M-phase was only 9% for GFP-SETX positive cells versus 19% for GFP-negative cells. This represents a highly significant difference in cell cycle progression ($P < .0001$ by χ^2 analysis). Hence, redistribution of fibrillarin and B23 from the nucleolus to the nucleoplasm upon SETX over-expression is likely due to a block in cell-cycle progression at S-phase [18].

4. Discussion

SETX is critical to neuron survival, as both recessive and dominant mutations result in neurodegenerative disease. In addition, SETX biology is also important to age-related maintenance of genome stability.

Despite its large size, GFP-tagged SETX can be effectively transfected into Hek293 cells, where it localized to the nucleoplasm as previously shown [18]. However, transfection of Flag- and GFP-tagged SETX had a dramatic effect on the localization of two prominent markers of the nucleolus, fibrillarin and B23, which were redistributed to the nucleoplasm in the vast majority of transfected cells. In GFP-SETX transfected cells, the appearance was typical of prophase nucleolus disassembly [31]. We found no evidence to support nucleolus toxicity or a general induction of apoptosis mediated cell death. But it is interesting to note that previous studies with Sen1p, the yeast orthologue to SETX: that inactivation of Sen1p by temperature shift of a strain carrying sen1-1 leads to mislocalization of two nucleolar proteins, Nop1 (yeast fibrillarin) and Ssb1 [32]. To investigate our hypothesis that SETX over-expression induced cell-cycle arrest, we employed flow cytometry and found that indeed GFP-SETX positive cells showed a clear shift from the normal bimodal distribution in cycling cells (G_1, S-phase, G_2/M), to a pattern characteristic of S-phase arrest [33]. In addition, we found that a functional SETX helicase domain was required to induce S-phase arrest, as deletion of the P-Loop GTP/ATP binding motif completely abolished the effect.

The SETX helicase is known to form S/G_2 phase foci where it is thought to direct incomplete RNA transcripts to the nuclear exosome for degradation [20], particularly at sites of DNA pol – RNAP II collision [18]. In addition, the DNA damage response proteins with which SETX may interact are poorly understood. Thus, upon even modest protein level elevation, SETX may sequester essential proteins that trigger S-phase arrest. Our confocal microscopy and FACS analysis demonstrate that once functional SETX protein is raised beyond a minimum threshold, S-phase arrest is induced. But due to the overt effect that transfected SETX has on an individual cell basis, combined with the reduced transfection efficiency, it remains technically difficult to define the specific level of SETX elevation required to induce S-phase arrest. This phenomenon may reflect SETX's role at S/G_2 phase foci, which strongly co-localize with 53BP1 and γH2AX, two protein markers of spontaneous DNA lesions and transcriptionally active nuclear bodies [18].

We and others have previously demonstrated SETX-exosome interactions [19, 20], and directing nascent RNAs to the nuclear exosome at S-phase foci may be critically important. This process may be highly sensitive to SETX protein levels, potentially explaining its tight regulation. Although such processes are obviously crucial for cycling cells, how would SETX-exosome interactions affect neurons? As it turns out, RNAP II undergoes self-collision in regions where positive and negative strand transcription overlaps [21]. Regulation of convergent transcription in neurons might be sensitive to defects in SETX function, or expression levels. In neurons, where long transcripts are known to be enriched [34], RNAP II self-collisions would occur more frequently, underscoring a potentially key role for SETX function that may be linked with disease.

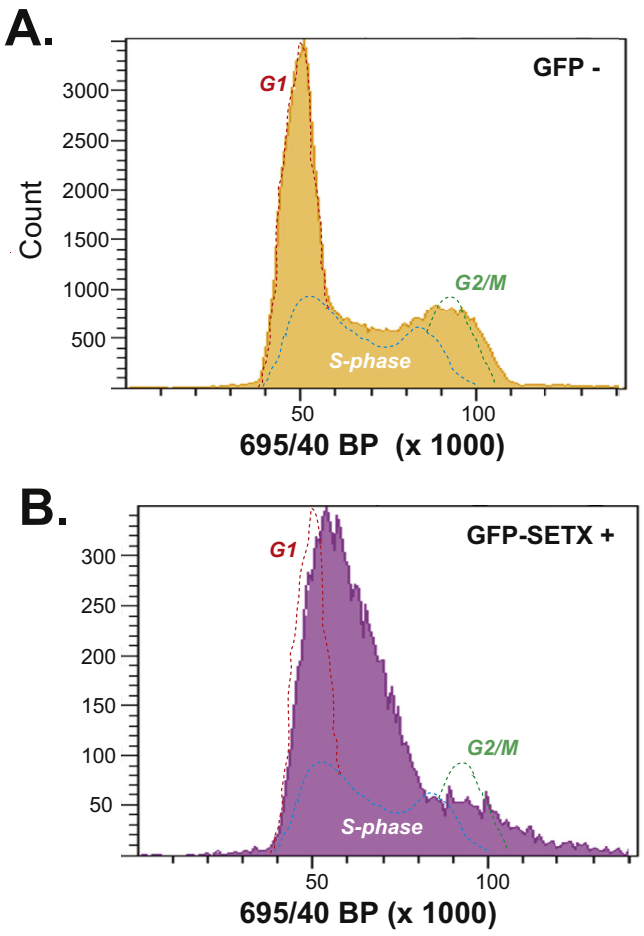

Figure 4. SETX over-expression in HEK293A cells causes S-phase cell-cycle arrest. We analyzed 133,759 total events sorted from GFP-SETX transfected HEK293A cells and removed cell debris and doubles with forward-scatter and side-scatter gating to isolate single viable cells (107,136). The FITC-A signal cut-off to define GFP-negative cells (GFP-) was defined from non-transfected HEK293A controls. (A) The PI signal (695/40 BP) was plotted for 70,869 GFP- cells from the GFP-SETX transfection. This histogram shows a typical distribution of cycling-cells, with the highest cell count representing G_1 cells (*47%*), a smaller peak for cells in G_2/Mitosis (*19%*) and a partially overlapping S-phase cells (*34%*). (B) 10,000 GFP-positive cells (GFP+) were gated and PI signal was plotted. The GFP-SETX + cells show a very large shift from G_1 (*29%*) into S-phase (*62%*), which largely do not enter G_2/M-phase (*9%*). We performed Chi-squared analysis, and found that the results were highly significant ($\chi^2 > 2961.5$; $P < 0.0001$).

Declarations

Author contribution statement

Craig L. Bennett: Conceived and designed the experiments; Performed the experiments; Analyzed and interpreted the data; Wrote the paper.

Bryce L. Sopher: Contributed reagents, materials, analysis tools or data.

Albert R. La Spada: Analyzed and interpreted the data; Wrote the paper.

Funding statement

This work was supported by the US National Institutes of Health (R01 NS100023 [A.R.L.S.]), and the Robert Packard Center for ALS Research at Johns Hopkins [A.R.L.S.].

Competing interest statement

The authors declare no conflict of interest.

Additional information

No additional information is available for this paper.

References

[1] The Human Gene Mutation Database.
[2] M.F. Lavin, Y. Shiloh, The genetic defect in ataxia-telangiectasia, Annu. Rev. Immunol. 15 (1997) 177–202.
[3] D.R. Lynch, C.D. Braastad, N. Nagan, Ovarian failure in ataxia with oculomotor apraxia type 2, Am. J. Med. Genet. 143 (2007) 1775–1777.
[4] M. Anheim, B. Monga, M. Fleury, P. Charles, C. Barbot, M. Salih, J.P. Delaunoy, M. Fritsch, L. Arning, M. Synofzik, L. Schols, J. Sequeiros, C. Goizet, C. Marelli, I. Le Ber, J. Koht, J. Gazulla, J. De Bleecker, M. Mukhtar, N. Drouot, L. Ali-Pacha, T. Benhassine, M. Chbicheb, A. M'Zahem, A. Hamri, B. Chabrol, J. Pouget, R. Murphy, M. Watanabe, P. Coutinho, M. Tazir, A. Durr, A. Brice, C. Tranchant, M. Koenig, Ataxia with oculomotor apraxia type 2: clinical, biological and genotype/phenotype correlation study of a cohort of 90 patients, Brain 132 (2009) 2688–2698.
[5] Y.Z. Chen, C.L. Bennett, H.M. Huynh, I.P. Blair, I. Puls, J. Irobi, I. Dierick, A. Abel, M.L. Kennerson, B.A. Rabin, G.A. Nicholson, M. Auer-Grumbach, K. Wagner, P. De Jonghe, J.W. Griffin, K.H. Fischbeck, V. Timmerman, D.R. Cornblath, P.F. Chance, DNA/RNA helicase gene mutations in a form of juvenile amyotrophic lateral sclerosis (ALS4), Am. J. Hum. Genet. 74 (2004) 1128–1135.
[6] B.A. Rabin, J.W. Griffin, B.J. Crain, M. Scavina, P.F. Chance, D.R. Cornblath, Autosomal dominant juvenile amyotrophic lateral sclerosis, Brain 122 (1999) 1539–1550.
[7] F. Avemaria, C. Lunetta, C. Tarlarini, L. Mosca, E. Maestri, A. Marocchi, M. Melazzini, S. Penco, M. Corbo, Mutation in the senataxin gene found in a patient affected by familial ALS with juvenile onset and slow progression, Amyotroph Lateral Scler. 12 (2011) 228–230.
[8] S. Rudnik-Schoneborn, L. Arning, J.T. Epplen, K. Zerres, SETX gene mutation in a family diagnosed autosomal dominant proximal spinal muscular atrophy, Neuromuscul. Disord. 22 (2012) 258–262.
[9] P.F. Chance, B.A. Rabin, S.G. Ryan, Y. Ding, M. Scavina, B. Crain, J.W. Griffin, D.R. Cornblath, Linkage of the gene for an autosomal dominant form of juvenile amyotrophic lateral sclerosis to chromosome 9q34, Am. J. Hum. Genet. 62 (1998) 633–640.
[10] I. Le Ber, N. Bouslam, S. Rivaud-Pechoux, J. Guimaraes, A. Benomar, C. Chamayou, C. Goizet, M.C. Moreira, S. Klur, M. Yahyaoui, Y. Agid, M. Koenig, G. Stevanin, A. Brice, A. Durr, Frequency and phenotypic spectrum of ataxia with oculomotor apraxia 2: a clinical and genetic study in 18 patients, Brain 127 (2004) 759–767.
[11] Y. Weng, K. Czaplinski, S.W. Peltz, Genetic and biochemical characterization of mutations in the ATPase and helicase regions of the Upf1 protein, Mol. Cell Biol. 16 (1996) 5477–5490.
[12] K. Grohmann, M. Schuelke, A. Diers, K. Hoffmann, B. Lucke, C. Adams, E. Bertini, H. Leonhardt-Horti, F. Muntoni, R. Ouvrier, A. Pfeufer, R. Rossi, L. Van Maldergem, J.M. Wilmshurst, T.F. Wienker, M. Sendtner, S. Rudnik-Schoneborn, K. Zerres, C. Hubner, Mutations in the gene encoding immunoglobulin mu-binding protein 2 cause spinal muscular atrophy with respiratory distress type 1, Nat. Genet. 29 (2001) 75–77.
[13] H.E. Mischo, B. Gomez-Gonzalez, P. Grzechnik, A.G. Rondon, W. Wei, L. Steinmetz, A. Aguilera, N.J. Proudfoot, Yeast Sen1 helicase protects the genome from transcription-associated instability, Mol. Cell. 41 (2011) 21–32.
[14] K. Skourti-Stathaki, N.J. Proudfoot, N. Gromak, Human senataxin resolves RNA/DNA hybrids formed at transcriptional pause sites to promote xrn2-dependent termination, Mol. Cell. 42 (2011) 794–805.
[15] A.J. Yeo, O.J. Becherel, J.E. Luff, J.K. Cullen, T. Wongsurawat, P. Jenjaroenpoon, V.A. Kuznetsov, P.J. McKinnon, M.F. Lavin, R-loops in proliferating cells but not in the brain: implications for AOA2 and other autosomal recessive ataxias, PLoS One 9 (2014), e90219.
[16] A. Banerjee, M.C. Sammarco, S. Ditch, J. Wang, E. Grabczyk, A novel tandem reporter quantifies RNA polymerase II termination in mammalian cells, PLoS One 4 (2009), e6193.
[17] C.L. Bennett, A.R. La Spada, Unwinding the role of senataxin in neurodegeneration, Discov. Med. 19 (2015) 127–136.
[18] O. Yuce, S.C. West, Senataxin, defective in the neurodegenerative disorder ataxia with oculomotor apraxia 2, lies at the interface of transcription and the DNA damage response, Mol. Cell Biol. 33 (2013) 406–417.
[19] C.L. Bennett, Y. Chen, M. Vignali, R.S. Lo, A.G. Mason, A. Unal, N.P. Huq Saifee, S. Fields, A.R. La Spada, Protein interaction analysis of senataxin and the ALS4 L389S mutant yields insights into senataxin post-translational modification and uncovers mutant-specific binding with a brain cytoplasmic RNA-encoded peptide, PLoS One 8 (2013), e78837.
[20] P. Richard, S. Feng, J.L. Manley, A SUMO-dependent interaction between Senataxin and the exosome, disrupted in the neurodegenerative disease AOA2, targets the exosome to sites of transcription-induced DNA damage, Genes Dev. 27 (2013) 2227–2232.
[21] D.J. Hobson, W. Wei, L.M. Steinmetz, J.Q. Svejstrup, RNA polymerase II collision interrupts convergent transcription, Mol. Cell. 48 (2012) 365–374.
[22] M. Polymenidou, C. Lagier-Tourenne, K.R. Hutt, S.C. Huelga, J. Moran, T.Y. Liang, S.C. Ling, E. Sun, E. Wancewicz, C. Mazur, H. Kordasiewicz, Y. Sedaghat, J.P. Donohue, L. Shiue, C.F. Bennett, G.W. Yeo, D.W. Cleveland, Long pre-mRNA depletion and RNA missplicing contribute to neuronal vulnerability from loss of TDP-43, Nat. Neurosci. 14 (2011) 459–468.
[23] M. Beck, A. Schmidt, J. Malmstroem, M. Claassen, A. Ori, A. Szymborska, F. Herzog, O. Rinner, J. Ellenberg, R. Aebersold, The quantitative proteome of a human cell line, Mol. Syst. Biol. 7 (2011) 549.
[24] D.J. DeMarini, F.R. Papa, S. Swaminathan, D. Ursic, T.P. Rasmussen, M.R. Culbertson, M. Hochstrasser, The yeast SEN3 gene encodes a regulatory subunit of the 26S proteasome complex required for ubiquitin-dependent protein degradation in vivo, Mol. Cell Biol. 15 (1995) 6311–6321.
[25] C.L. Bennett, S.G. Dastidar, S.C. Ling, B. Malik, T. Ashe, M. Wadhwa, D.B. Miller, C. Lee, M.B. Mitchell, M.A. van Es, C. Grunseich, Y. Chen, B.L. Sopher, L. Greensmith, D.W. Cleveland, A.R. La Spada, Senataxin mutations elicit motor neuron degeneration phenotypes and yield TDP-43 mislocalization in ALS4 mice and human patients, Acta Neuropathol. 136 (2018) 425–443.
[26] Y.Z. Chen, S.H. Hashemi, S.K. Anderson, Y. Huang, M.C. Moreira, D.R. Lynch, I.A. Glass, P.F. Chance, C.L. Bennett, Senataxin, the yeast Sen1p orthologue: characterization of a unique protein in which recessive mutations cause ataxia and dominant mutations cause motor neuron disease, Neurobiol. Dis. 23 (2006) 97–108.
[27] R.H. Roda, C. Rinaldi, R. Singh, A.B. Schindler, C. Blackstone, Ataxia with oculomotor apraxia type 2 fibroblasts exhibit increased susceptibility to oxidative DNA damage, J. Clin. Neurosci. Offic. J. Neurosurg. Soc. Aust. 21 (2014) 1627–1631.
[28] I. Kwon, S. Xiang, M. Kato, L. Wu, P. Theodoropoulos, T. Wang, J. Kim, J. Yun, Y. Xie, S.L. McKnight, Poly-dipeptides encoded by the C9orf72 repeats bind nucleoli, impede RNA biogenesis, and kill cells, Science 345 (2014) 1139–1145.
[29] Z. Tao, H. Wang, Q. Xia, K. Li, K. Li, X. Jiang, G. Xu, G. Wang, Z. Ying, Nucleolar stress and impaired stress granule formation contribute to C9orf72 RAN translation-induced cytotoxicity, Hum. Mol. Genet. 24 (2015) 2426–2441.
[30] Z. Yao, S. Duan, D. Hou, W. Wang, G. Wang, Y. Liu, L. Wen, M. Wu, B23 acts as a nucleolar stress sensor and promotes cell survival through its dynamic interaction with hnRNPU and hnRNPA1, Oncogene 29 (2010) 1821–1834.
[31] D. Hernandez-Verdun, Assembly and disassembly of the nucleolus during the cell cycle, Nucleus 2 (2011) 189–194.
[32] D. Ursic, D.J. DeMarini, M.R. Culbertson, Inactivation of the yeast Sen1 protein affects the localization of nucleolar proteins, Mol. Gen. Genet. 249 (1995) 571–584.
[33] Z. Shi, A. Azuma, D. Sampath, Y.X. Li, P. Huang, W. Plunkett, S-Phase arrest by nucleoside analogues and abrogation of survival without cell cycle progression by 7-hydroxystaurosporine, Canc. Res. 61 (2001) 1065–1072.
[34] C. Lagier-Tourenne, M. Polymenidou, K.R. Hutt, A.Q. Vu, M. Baughn, S.C. Huelga, K.M. Clutario, S.C. Ling, T.Y. Liang, C. Mazur, E. Wancewicz, A.S. Kim, A. Watt, S. Freier, G.G. Hicks, J.P. Donohue, L. Shiue, C.F. Bennett, J. Ravits, D.W. Cleveland, G.W. Yeo, Divergent roles of ALS-linked proteins FUS/TLS and TDP-43 intersect in processing long pre-mRNAs, Nat. Neurosci. 15 (2012) 1488–1497.